Nuclear Physics B344 (1990) 627–645
North-Holland

ON THE REMARKABLE STRUCTURE OF THE SUPERCONDUCTING INTERMEDIATE STATE

David J.E. CALLAWAY *

Department of Physics, The Rockefeller University, 1230 York Avenue, New York, NY 10021, USA

Received 19 December 1989

If a large square plate of a type I superconductor is placed in a perpendicular magnetic field, the field will penetrate it in a pattern of domains. The intermediate-state problem is to predict this pattern. In the critical Ginzburg–Landau theory, the horizontal and vertical directions of the plate are essentially Fourier conjugate coordinates, like position and momentum in quantum mechanics. Thus, the intermediate state allows us a rare direct glimpse of quantum phase space. It is also demonstrated that, although Landau's (1937) textbook model is inconsistent with the Ginzburg–Landau equations, its qualitative nature is correct. Elongated structures consistent with a complete spontaneous breakdown of discrete rotational invariance are predicted. Comments with regard to lattice Higgs simulations are also made.

1. Prolegomena

The problem of the magnetic intermediate state in superconductors is both extremely fascinating and extraordinarily difficult. Its solution involves the analysis of highly degenerate ground states and intricate fractal-like patterns on many length scales (cf. sect. 7) and utilizes arcane mathematical structures that are most familiar perhaps to the string theorist. Yet, for all the complexity of its solution, the problem itself can be stated with deceptive ease: Consider a block of type I superconducting material placed in a weak magnetic field. Because of the Meissner effect the magnetic field is expelled. As the field strength is increased the magnetic field penetrates the superconductor. The problem is to predict this pattern of penetration.

2. Background and synopsis

The simplest illustration of the magnetic intermediate state is a problem originally addressed by Landau [1] and considered in detail here. Landau's prob-

* Work supported in part by the US Department of Energy under contract no. DE-AC02-87ER40325-Task B_1.

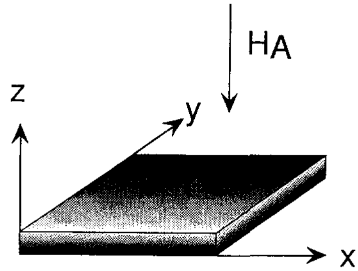

Fig. 1. Geometry of problem. Magnetic field is incident in $\hat{z}$ direction, and is a constant $|H| = H_A$ at large z.

lem involved a large square plate of a (type I) superconductor in a perpendicular magnetic field. Landau predicted that the magnetic field would penetrate the plate in a periodic series of stripes. Following fig. 1, we take the plate to lie in the xy plane. Then the pattern predicted by Landau is independent of y and periodic in x (or vice-versa), consistent with a complete spontaneous breaking of the *discrete* $[x \leftrightarrow y]$ rotational symmetry of the system.

Subsequent experimental work [2] revealed that the true situation was far more baroque, involving complex patterns on many length scales. Usually, these patterns include elongated structures, indicating that Landau's picture might be a qualitative guide to the nature of the intermediate state. Indeed, if the magnetic field is applied at a slightly *oblique* angle, the domain patterns found [3] do in fact resemble Landau's model.

Before we are too critical of this early attempt of Landau, it is well to remember that, at the time (1937) of his analysis, superconductivity was even less well-understood than it is today. Most significantly, his analysis predated the Ginzburg–Landau equations (1950) [4] and thus Abrikosov's germinal work [5] which first distinguished between type I and type II superconductors. Landau's model was *au fond* an exercise in classical electromagnetism, augmented with phenomenological boundary conditions obtained via the Meissner effect.

By contrast, the analysis presented here is based upon the Ginzburg–Landau equations, following and extending the classic works of Abrikosov [5] and others [6, 7]. It proceeds by expanding these equations in a perturbation series about the critical magnetic field above which the superconducting wave function vanishes. A more complete analysis of the problem probably requires numerical techniques, such as those presently applied to lattice Higgs models [8]. (In anticipation of such calculations [9], some remarks pertinent to lattice simulations are included below.) Nevertheless, even within this insular perturbative domain startling results can be obtained. At scales larger than the coherence length, the superconductor behaves as if the x- and y-directions were Fourier conjugate coordinates, like position and momentum in a one-dimensional quantum mechanical problem (cf. fig. 1). Thus, the discrete $[x \leftrightarrow y]$ rotation symmetry is unlikely, for only rarely does a wave function equal its Fourier transform. Indeed, the perturbative solutions to the Ginzburg–Landau equations are generally elongated shapes, in *qualitative* agreement with Landau's construction. From the Fourier conjugation property mentioned above the *quantitative* fallacy of Landau's model can also be seen. If the flux patterns are independent of, say, the y-coordinate, then the superconducting wave function must be an (unlocalized) plane wave in the y-direction. The Fourier transform of a plane wave is a delta function, so the wave function will be sharply localized in the x-coordinate, and not the periodic function envisaged by Landau.

3. Landau's problem revisited

Following Ginzburg and Landau [4], we assume that the free energy density $f(\boldsymbol{x})$ of the system can be expanded as

$$f(\boldsymbol{x}) = f_{\mathrm{n}} + \alpha|\psi(\boldsymbol{x})|^2 + \tfrac{1}{2}\beta|\psi(\boldsymbol{x})|^4 + \frac{1}{2m^*}\left|\left(\frac{\hbar}{i}\partial - \frac{e^*}{c}\boldsymbol{A}\right)\psi(\boldsymbol{x})\right|^2 + \frac{1}{4\pi}\tilde{H}^2, \quad (1)$$

where f_{n} is the free energy of the normal material, $\psi(\boldsymbol{x})$ is the order parameter (i.e., the superconducting wave function), $\boldsymbol{H}$ is the magnetic field, and the rest are phenomenological parameters. (It should be pointed out that this formalism is very general [10] and can be derived [11] from the BCS theory.) This equation can be rescaled to as to measure

$$\psi(\boldsymbol{x}) \text{ in units of } |\psi_\infty| = \left(\frac{-\alpha}{2\beta}\right)^{1/2}, \quad (2a)$$

$$\boldsymbol{x} \text{ in units of } \xi = \frac{\hbar}{\sqrt{-2m\alpha}}, \quad (2b)$$

$$f(\boldsymbol{x}) - f_{\mathrm{n}} \text{ in units of } -2\alpha|\psi_\infty|^2, \quad (2c)$$

$$A(\boldsymbol{x}) \text{ in units of } \Phi_0/2\pi\xi, \quad (2d)$$

where $\Phi_0 = 2\pi\hbar/e^*$ is the elementary flux quantum, and ξ is the coherence length. Also, we define

$$\lambda_\infty \equiv \frac{m^*c^2}{4\pi|\psi_\infty|^2 e^{*2}}, \quad (3a)$$

$$\kappa^2 \equiv \lambda_\infty^2/\xi^2, \quad (3b)$$

whence

$$f(\boldsymbol{x}) - f_{\mathrm{n}} = \tfrac{1}{2}|\boldsymbol{D}\psi|^2 + \tfrac{1}{4}\left(|\psi(\boldsymbol{x})|^2 - 1\right)^2 + \tfrac{1}{2}\kappa^2 \boldsymbol{H}^2 , \tag{4}$$

where $\boldsymbol{D} = \partial - i\boldsymbol{A}$ is the covariant derivative. The corresponding Euler equations of motion are

$$\boldsymbol{D}^2\psi + \psi - |\psi|^2\psi = 0 , \tag{5a}$$

$$-\kappa^2\left[\partial^2\boldsymbol{A} - \partial(\partial\cdot\boldsymbol{A})\right] = \mathrm{Im}[\psi^*\boldsymbol{D}\psi] . \tag{5b}$$

Note the appearance of the Abrikosov parameter κ. The value of κ determines [5] whether the superconductor is type I ($\kappa < 1/\sqrt{2}$) or type II ($\kappa > 1/\sqrt{2}$). Here the primary concern is type I superconductors, for which the superconducting/normal domain wall energy parameter is *positive*. Thus the domain surface area is typically minimized in equilibrium configurations.

Consider (see fig. 1) Landau's problem of a large flat square plate of type I superconductor in the *xy* plane with a constant magnetic field incident in the $\hat{z}$-direction. Deep inside the plate and away from the edges the magnetic field $\boldsymbol{H}$ has only a $\hat{z}$ component. If the thickness of the plate is much greater than the coherence length ξ (which ranges from 500 to 10000 Angstroms for typical pure superconductors) then inside the plate $\boldsymbol{H}$ will be essentially independent of z. Thus

$$\boldsymbol{H} = H(x, y)\hat{e}_z . \tag{6}$$

The symmetry of the problem then permits the choice

$$\boldsymbol{A} = A(x, y)\hat{e}_y . \tag{7}$$

The Ginzburg–Landau equations (5) are to be solved in a perturbative expansion around the critical region where $|\boldsymbol{H}| \approx H_{\mathrm{c}}$ (which equals one in the present units). In this regime the order parameter $\psi(\boldsymbol{x})$ is small, so eqs. (5) can be linearized

$$\left(\boldsymbol{D}_0^2 + 1\right)\psi(\boldsymbol{x}) = 0 , \tag{8a}$$

where

$$\boldsymbol{D}_0 \equiv \partial + iH_{\mathrm{A}}x\hat{e}_y , \tag{8b}$$

and H_{A} is a constant equal to the magnitude of the applied magnetic field.

Eqs. (8) are easily solved by separating variables, i.e.

$$\psi(\boldsymbol{x}) = \mathrm{e}^{-iky} r(\boldsymbol{x}), \tag{9a}$$

$$\left\{\partial_x^2 + \left[1 - H_\mathrm{A}^2(x - k/H_\mathrm{A})^2\right]\right\} r(x) = 0. \tag{9b}$$

Note that eq. (9b) is essentially the Schrödinger equation for one-dimensional harmonic oscillator, with an important difference–the "energy" E equals one! Away from the xy edges of a large plate, the appropriate solutions for $\psi(\boldsymbol{x})$ are the familiar normalizable eigenfunctions, whence

$$(2n+1) H_\mathrm{A} = 1, \tag{10}$$

and thus $H_\mathrm{A} \leqslant H_\mathrm{c} = 1$. The seeming quantization of H_A is an artifact of the linearized analysis [see eq. (54) et seq.]. Thus, it is necessary to include the nonlinear terms (at least perturbatively) when H_A is less than H_c.

The appropriate solution to the linearized Ginzburg–Landau equation for $H_\mathrm{A} = H_\mathrm{c} = 1$ is thus

$$\psi(x, y) = \int \mathrm{d}k \exp\left[-iky - \tfrac{1}{2}(x-k)^2\right] C(k), \tag{11}$$

where the function $C(k)$ is arbitrary in this limit. Recall that Landau's model predicts that $|\psi(x, y)|^2$ is independent of y and periodic in x (or vice-versa). But this would mean that

$$C(k) \sim \delta(k - k_0), \tag{12a}$$

so that

$$|\psi(x, y)|^2 \sim \mathrm{e}^{-(x-k_0)^2}, \tag{12b}$$

which is clearly not periodic in x. Thus, in the strictest sense Landau's construction is (oddly enough) inconsistent with the Ginzburg–Landau equations. This inconsistency persists in the full nonlinear case.

The present analysis proceeds as follows. First, various interesting properties of the wave functions eq. (11) are adumbrated. Following this general discussion it will be shown how the nonlinear terms in the Ginzburg–Landau theory serve to constrain the function $C(k)$ in eq. (11). Several observations about the allowed solution space will then be made.

4. The remarkable structure of the wave function: A glimpse of quantum phase space

One rather striking property of the wave function in the critical region follows directly from eq. (11). We construct $\rho_1(x)$, the density in x of the order parameter

$$\rho_1(x) \equiv \int_{-\infty}^{\infty} |\psi(x, y)|^2 \, \mathrm{d}y , \tag{13a}$$

$$= 2\pi \int \mathrm{d}k |C(k)|^2 \, \mathrm{e}^{-(x-k)^2} \tag{13b}$$

$$\equiv 2\pi^{3/2} \int \mathrm{d}k |C(k)|^2 \Delta(x-k) .$$

Similarly,

$$\rho_2(y) \equiv \int_{-\infty}^{\infty} |\psi(x, y)|^2 \, \mathrm{d}x , \tag{14a}$$

$$= 2\pi \int \mathrm{d}q |\tilde{C}(q)|^2 \, \mathrm{e}^{-(y-q)^2} \tag{14b}$$

$$\equiv 2\pi^{3/2} \int \mathrm{d}q |\tilde{C}(q)|^2 \Delta(y-q) ,$$

where

$$\tilde{C}(q) \equiv \int \frac{\mathrm{d}k}{\sqrt{2\pi}} \, \mathrm{e}^{-ikq} C(k) \tag{15}$$

is just the Fourier transform of $C(k)$, and

$$\Delta(s) \equiv \frac{1}{\sqrt{\pi}} \, \mathrm{e}^{-s^2} \tag{16}$$

is a sharply localized smearing function with unit volume.

Recall that distances here are measured in units of the coherence length, which is microscopically small. At macroscopic distances $\Delta(s) \to \delta(s)$, and

$$\rho_1(x) \approx 2\pi^{3/2} |C(x)|^2 , \tag{17a}$$

$$\rho_2(y) \approx 2\pi^{3/2} |\tilde{C}(y)|^2 . \tag{17b}$$

From eqs. (17) it is seen that at macroscopic scales, x and y can be thought of as (Fourier) conjugate coordinates, much like position and momentum in a one-dimensional quantum-mechanical problem. The function $C(x)$ plays the role of the position-space wavefunction in this quantum analogy, just as $\tilde{C}(y)$ corresponds to its momentum-space counterpart. Thus at macroscopic scales the intermediate state of a critical superconductor allows us a glimpse of a quantum "phase space".

This point is worthy of elaboration. Over a half-century ago Wigner proposed [12] a density function $P(x, p)$ for quantum phase-space. With a few changes of convention, this function is

$$P_{\psi}(x, p) = \frac{1}{\pi} \int \mathrm{d}s\, \mathrm{e}^{-2ips} \psi^*(x+s) \psi(x-s) . \tag{18}$$

The Wigner phase-space density possesses the following properties

$$\int P_{\psi}(x, p)\, \mathrm{d}p = |\psi(x)|^2 , \tag{19a}$$

$$\int P_{\psi}(x, p)\, \mathrm{d}x = |\tilde{\psi}(p)|^2 , \tag{19b}$$

as expected of a phase-space distribution. Compare the intermediate state result

$$|\psi(x, y)|^2 = 2\pi^{3/2} \int \mathrm{d}u\, \Delta(x-u) \int \mathrm{d}v\, \Delta(y-v) \frac{1}{\pi} \int \mathrm{d}s\, \mathrm{e}^{-2isv} C(u+s) C^*(u-s) \tag{20a}$$

$$= 2\pi^{3/2} \int \mathrm{d}u\, \Delta(x-u) \int \mathrm{d}v\, \Delta(y-v) P_{C^*}(u, v) . \tag{20b}$$

Except for microscopic smearing factors and unimportant conventions, eqs. (18) and (20) are identical if the coordinate y is exchanged for the momentum p. Thus, the squared intermediate-state wave function does behave like a phase-space density. More to the point, Wigner's phase-space distribution is not positive-definite, and so fails an important requirement of a probability distribution. The absolute square of a wave function is however positive-definite by construction. These points are reformulated more precisely below, where the intermediate state wavefunction is rewritten in terms of quantum lumps.

5. Can Landau be rescued?

As shown above, Landau's construction is generally inconsistent with the Ginzburg–Landau equations, which are very general and firmly founded. But we should not discard Landau's model prematurely. Let us therefore abstract two properties of Landau's construction and see if general solutions to the linearized Ginzburg–Landau equations can be found which satisfy these properties. Then in sect. 6 we will see how the nonlinear terms in the Ginzburg–Landau equations serve to refine the solution space. The properties we search for are:

(i) *Space-filling solutions*. The $|\psi|^2$ distribution fills the xy plane;

(ii) *Elongated structures*. Since Landau's construction is highly asymmetric we ask if $[x \leftrightarrow y]$ symmetry is an expected feature in the solution space.

5.1. SPACE-FILLING DISTRIBUTIONS: THE ABRIKOSOV SOLUTIONS

Consider (following Abrikosov [5]) the solutions $\psi(x, y)$ defined by eq. (11) with

$$C(k) = \sum_{n=-\infty}^{\infty} C_{n/p}\delta(k - nk_0), \tag{21a}$$

where k_0 is a real parameter and $C_{n/p}$ is periodic

$$C_{n/p} = C_{(n+p)/p}. \tag{21b}$$

Thus the $C_{n/p}$ can be specified by p independent complex parameters [15]. Then

$$\psi_p(x, y) = \sum_{n=-\infty}^{\infty} C_{n/p}\, e^{-ink_0y-(x-nk_0)^2/2} \tag{22}$$

obeys the relations

$$\psi_p(x, y + 2\pi/k_0) = \psi_p(x, y) \tag{23a}$$

$$\psi_p(x + pk_0, y) = e^{-ipk_0y}\, \psi_p(x, y). \tag{23b}$$

Thus $|\psi_p(x, y)|^2$ is *periodic* [and $\psi_p(x, y)$ is *quasi-periodic*] on a rectangle of dimension $(\Delta x, \Delta y) = (pk_0, 2\pi/k_0)$. This property ensures us that the wave function is *space-filling*. [Thus, for example the analysis of sect. 4 needs to be modified by replacing integrals like those in eq. (13) by spatial averages.] The functions $\psi_p(x, y)$ can also be written in terms of Jacobi theta functions, e.g.

$$\psi_1(x, y) = iC_0\, e^{-x^2/2}\Theta_3\left[ik_0(x - iy), e^{-k_0^2/2}\right]. \tag{24}$$

Since $|\psi_p(x, y)|^2$ is a periodic function, it is useful to consider its Fourier transform. Following Lasher [6] we write

$$|\psi_p(x, y)|^2 = N_p \sum_{\boldsymbol{k}} g_p(\boldsymbol{k}) e^{i\boldsymbol{k}\cdot\boldsymbol{r}}, \tag{25a}$$

where

$$N_p \equiv \overline{|\psi_p(x, y)|^2} \tag{25b}$$

is the xy spatial average of $|\psi_p(x, y)|^2$ [thus $g_p(0) = 1$]. The $C_{n/p}$ are normalized by

$$\sum_{n=0}^{p-1} |C_{n/p}|^2 = 1 . \tag{26}$$

Then it follows that

$$g_p(\boldsymbol{k}) = \mathrm{e}^{-\boldsymbol{k}^2/4 + ik_x k_y/2}\, h_p(N_x, N_y), \tag{27a}$$

$$h_p(N_x, N_y) = \sum_{n=0}^{p-1} \exp(2\pi i n N_x/p) C^*_{(n+N_y)/p} C_{n/p}, \tag{27b}$$

$$h_p(0,0) = 1, \tag{27c}$$

with the sum in eq. (25a) taken over values

$$\boldsymbol{k} = \left[(2\pi/pk_0) N_x, k_0 N_y\right], \tag{28}$$

where (N_x, N_y) are integers ranging from negative to positive infinity.

It is also useful to define $\tilde{C}_{m/p}$, the finite Fourier transform of $C_{n/p}$

$$\tilde{C}_{m/p} = \frac{1}{\sqrt{p}} \sum_{n=0}^{p-1} \mathrm{e}^{2\pi i m n/p} C_{n/p}, \tag{29}$$

whence

$$h_p(M, N) = \sum_{m,n=0}^{p-1} \mathrm{e}^{2\pi i (Mm + Nn)/p}\, \tilde{h}_p(m, n), \tag{30}$$

with

$$\tilde{h}_p(m, n) = \frac{1}{\sqrt{p}} \mathrm{e}^{2\pi i m n/p} C_{m/p} \tilde{C}^*_{n/p}, \tag{31}$$

which is periodic (with period p) in both m and n. By the Poisson sum rule, eq. (25a) can then be written

$$|\psi_p(x,y)|^2=\sqrt{2}\,N_p\sum_{m,n=-\infty}^{\infty}\tilde{h}_p(p-m,p-n)\phi(x-k_0m,y-2\pi n/k_0p)\,,\quad (32a)$$

$$\phi(x,y)\equiv\exp\left[-\tfrac{1}{2}(x^2+y^2)-ixy\right].\quad (32b)$$

Thus $|\psi_p|^2$ is simply a superposition of the quantum lumps ϕ, weighted by the periodic function $\tilde{h}_p$. The counterparts of eqs. (13) and (14) are

$$\sum_{m=0}^{p-1}\tilde{h}_p(m,n)=|\tilde{C}_n|^2\,,\quad (33a)$$

$$\sum_{n=0}^{p-1}\tilde{h}_p(m,n)=|C_m|^2\quad (33b)$$

and so

$$\sum_{m,n=0}^{p-1}\tilde{h}_p(m,n)=1\,.\quad (34)$$

Also

$$\sum_{m,n=0}^{p-1}|\tilde{h}_p(m,n)|^2=\frac{1}{p^2}\sum_{M,N=0}^{p-1}|h_p(M,N)|^2=\frac{1}{p}\,.\quad (35)$$

From eqs. (33) it is evident that $\tilde{h}_p(m,n)$ behaves like the Wigner function P_ψ of eq. (18), with $|C_{m/p}|^2$ and $|\tilde{C}_{n/p}|^2$, the complementary distributions in Fourier conjugate coordinates. Here m corresponds to the x-direction of the lump wave-function, while n corresponds to its y-direction. Clearly no "smearing factors" $\Delta(s)$ are present in eqs. (33). Thus, the quantum lump formation of the problem yields a more precise definition of the way in which the x and y coordinates act like Fourier conjugates.

5.2. ROTATIONAL SYMMETRY

By choosing wave functions $\psi_p(x,y)$ which obey eqs. (23), the square-plate Landau boundary conditions have implicitly been introduced. Thus, these solutions possess, at most, only a *discrete* $[x\leftrightarrow y]$ rotational invariance. When does this symmetry occur? From eqs. (28) and (31), it follows that $|\psi_p(x,y)|^2$ is $[x\leftrightarrow y]$

symmetric when

(i) $$k_0^2 = 2\pi/p \quad \text{and} \tag{36a}$$

(ii) $$\tilde{C}_{n/p} = e^{i\theta} C^*_{n/p}, \tag{36b}$$

with θ an arbitrary real parameter.

Consider further the structure of eq. (36b). It can be written as

$$\sum_{n=0}^{p-1} F_{mn} C_{n/p} = e^{i\theta} C^*_{m/p}, \tag{37a}$$

where

$$F_{mn} = \frac{1}{\sqrt{p}} e^{2\pi i\, mn/p}. \tag{37b}$$

The Fourier transform matrix F is symmetric and satisfies

$$F^4 = F^+ F = 1. \tag{38}$$

The eigenvectors $D_{n/p}(N)$ of F can be taken real, and the corresponding eigenvalues $\lambda_N = \exp(i\chi_N)$ are just the fourth roots of unity. Thus

$$C_{n/p} = e^{i(\theta - \chi_N)/2} D_{n/p}(N) \tag{39}$$

satisfies eq. (36b), and the problem of finding $[x \leftrightarrow y]$ symmetric functions $|\psi_p(x, y)|^2$ reduces to finding the eigenvectors of F. Linear combinations of the solutions eq. (39) with *real* coefficients also satisfy eq. (36b).

Some useful (unnormalized) eigenfunctions of F are tabulated below

$$\exp(i\chi_{\mathrm{I}}) = 1 : D_{n/p}(\mathrm{I}) = 1 + \delta_{n0}\sqrt{p}\,, \tag{40a}$$

$$\exp(i\chi_{\mathrm{II}}) = -1 : D_{n/p}(\mathrm{II}) = 1 - \delta_{n0}\sqrt{p}\,. \tag{40b}$$

It was pointed out by Lasher [6] that the order parameter $\psi^{(p)}(x, y)$ of a state consisting of only vortices of quantum number p can be written [cf. eq. (24)]

$$\psi^{(p)}(x, y) = \left[\psi_1\left(\frac{x}{\sqrt{p}}, \frac{y}{\sqrt{p}}\right)\right]^p. \tag{41}$$

The corresponding $C_{n/p}$ satisfy the recursion relation

$$C_{n/(p+1)} = \sum_{m=0}^{p-1} \exp\left\{ \frac{-k_0^2}{2p(p+1)} [(1+p)m - pn]^2 \right\} C_{m/p} . \tag{42}$$

When $k_0^2 = 2\pi$, the $C_{n/p}$ defined by eq. (42) are eigenfunctions $D_{n/p}(\mathrm{III})$ of F with eigenvalue $\exp(i\chi_{\mathrm{III}}) = 1$. (This is obvious, since powers of an $[x \leftrightarrow y]$ symmetric function are also symmetric.)

A fourth symmetric solution can be obtained from

$$A_{n/p}(s) \equiv \sum_{N=-\infty}^{\infty} \exp\left[-\frac{s^2}{2}\left(N - \frac{n}{p}\right)^2 \right] \tag{43a}$$

$$= \frac{\sqrt{2\pi}}{s} \sum_{M=-\infty}^{\infty} \exp\left[-\frac{2\pi^2}{s^2} M^2 - 2\pi i \frac{Mn}{p} \right], \tag{43b}$$

where eq. (43b) follows from eq. (43a) by application of the Poisson sum rule. The finite Fourier transform of $A_{n/p}(s)$ is

$$\tilde{A}_{n/p}(s) = \frac{\sqrt{2\pi p}}{s} A_{n/p}\left(\frac{2\pi p}{s}\right), \tag{44}$$

so that

$$D_{n/p}(\mathrm{IV}) = A_{n/p}\left(\sqrt{2\pi p}\right) \tag{45}$$

is an eigenvector of F with eigenvalue $\exp(i\chi_{\mathrm{IV}}) = 1$. More generally,

$$D_{n/p} = \int \mathrm{d}s \left[A_{n/p}(s) \pm \frac{\sqrt{2\pi p}}{s} A_{n/p}\left(\frac{2\pi p}{s}\right) \right] f(s) \tag{46}$$

[with $f(s)$ arbitrary] gives eigenvectors of F with eigenvalues $\mathrm{e}^{i\chi} = \pm 1$, respectively.

6. Constraining the wave function by including nonlinear effects

The above analysis concerned only the solution to the linearized Ginzburg–Landau equations. This solution space can be refined by including nonlinear terms in the analysis in a perturbative fashion. The most elegant way to do this is to express the wave function ψ and magnetic field $\boldsymbol{H}$ in a power series in a fictitious parameter ε [6]

$$\boldsymbol{H} = \boldsymbol{H}_0 + \varepsilon \boldsymbol{H}_1 + \varepsilon^2 \boldsymbol{H}_2 + \dots , \tag{47a}$$

$$\psi = \sqrt{\varepsilon}\left(\psi_0 + \varepsilon\psi_1 + \varepsilon^2\psi_2 + \dots\right) \tag{47b}$$

and then evaluate the free energy. At the end of the calculation, the parameter ε is set to one, and the corrected free energy is then minimized. The following derivation of eq. (56) is a recast version of the analysis of Abrikosov and others [5–7].

If the Euler equation eq. (5a) is multiplied by ψ^* and integrated over all space, the result is

$$\overline{\psi^* D^2 \psi + |\psi|^2 - |\psi|^4} = 0 , \tag{48}$$

where the bar (here and below) denotes an xy spatial average. Eq. (48) is integrated by parts and inserted into the Ginzburg–Landau free energy to yield

$$F = \overline{f(\boldsymbol{x})} - f_n = \tfrac{1}{2}\overline{\left(\kappa^2 H^2 + \tfrac{1}{2} - \tfrac{1}{2}|\psi|^4\right)}$$

$$\equiv F_0 + \varepsilon F_1 + \varepsilon^2 F_2 + \dots . \tag{49a}$$

At large $|z|$ (outside the plate) the magnetic field approaches a uniform constant value $|\boldsymbol{H}| \to H_{\mathrm{A}}$. Deep within the plate and away from the edges

$$\boldsymbol{A} = \hat{e}_y A(x, y) , \qquad -\boldsymbol{H} = \hat{e}_z H(x, y) . \tag{50a,b}$$

Only the first two terms of eq. (47a) are needed to evaluate the first correction to the free energy. Thus

$$H_0 = H_{\mathrm{c}} = 1 , \tag{51a}$$

$$H_1 = H_{\mathrm{A}} - H_{\mathrm{c}} - \frac{1}{2\kappa^2}\left(|\psi_0|^2 - \overline{|\psi_0|^2}\right), \tag{51b}$$

where ψ_0 is the lowest-order wave function (discussed in subsect. 5.1). The incident magnetic flux per unit area, B, is given by

$$B = \overline{H} = H_{\mathrm{c}} + \varepsilon(H_{\mathrm{A}} - H_{\mathrm{c}}) , \tag{52a}$$

$$\overline{H}_n \equiv 0 , \quad n > 1 , \tag{52b}$$

where eq. (52b) is chosen by convention. If eqs. (51) are substituted into eqs. (49), the result is

$$F_0 = \tfrac{1}{4} + \tfrac{1}{2}\kappa^2 H_c^2\,, \tag{53a}$$

$$F_1 = \kappa^2 H_c (H_A - H_c)\,, \tag{53b}$$

$$F_2 = \overline{\tfrac{1}{2}\kappa^2 H_1^2 - \tfrac{1}{4}|\psi_0|^4 + \kappa^2 H_0 H_2} \tag{53c}$$

$$= \tfrac{1}{2}\kappa^2 (H_A - H_c)^2 + \frac{1}{8\kappa^2}\left[(1-2\kappa^2)\overline{|\psi_0|^4} - \left(\overline{|\psi_0|^2}\right)^2\right]. \tag{53d}$$

There is a constraint equation which can be derived by expanding eq. (48) in powers of ε (Abrikosov [5] gives a different derivation)

$$\overline{|\psi_0|^2} = \frac{H_c - H_A}{1 + (2\kappa^2 - 1)\beta}\,, \tag{54}$$

where

$$\beta = \overline{|\psi_0|^4}\left(\overline{|\psi_0|^2}\right)^{-2} \tag{55}$$

is explicitly independent of B and the normalization of ψ_0. [Eq. (54) is just the next-order correction to eq. (10)]. Then up to second order in ε [5]

$$F = \tfrac{1}{4} + \tfrac{1}{2}\kappa^2 B^2 - \tfrac{1}{2}\kappa^2 \frac{(B-1)^2}{1 + (2\kappa^2 - 1)\beta}\,, \tag{56}$$

where B is measured in units of H_c.

The order ε^3 term has been evaluated by Lasher [6] for certain special cases. He found it to be proportional to $(2\kappa^2 - 1)$, thus presumably becoming small in the limit $\kappa \to 1/\sqrt{2}$ where our interest lies (see also ref. [16]).

Recall that Abrikosov's analysis concerned type II superconductors (where $\kappa > 1/\sqrt{2}$). When κ exceeds $1/\sqrt{2}$ the free energy eq. (18) is minimized by making β as small as possible ($\beta_{\min} \sim 1.16$). This leads to the standard prediction [5] of a triangular-lattice array of vortices for a type II superconductor. The present analysis goes *beyond* Abrikosov to look at $\kappa < 1/\sqrt{2}$, for which the minimum free energy occurs when

$$\beta \lesssim 1/(1 - 2\kappa^2)\,. \tag{57}$$

Note therefore that when $\kappa \lesssim 1/\sqrt{2}$ (as occurs in e.g. lead), β can be quite large. Also note that there is no real singularity in the free energy eq. (56) near this value, for eq. (54) implies that then B must be near its critical value of unity in order that there be a finite density of superconductor in the plate.

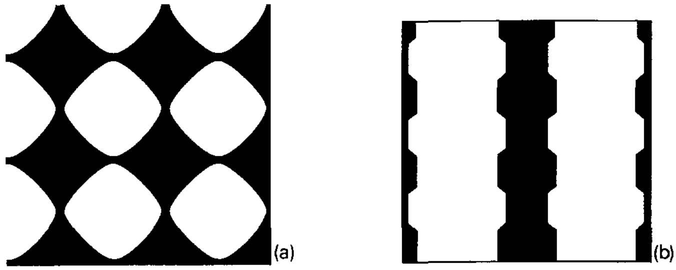

Fig. 2. Flux pattern generated by superconductor density $|\psi_1(x, y)|^2$. Shaded areas indicate where density exceeds 0.7 of its maximum: (a) $k_0 = \sqrt{2\pi}$; (b) $k_0 = 1.3\sqrt{2\pi}$.

The simplest example to consider is $\psi_1\ (x, y)$ [cf. eq. (22)]. Then

$$\beta_1 = g(k_0) g(2\pi/k_0), \tag{58a}$$

$$g(x) \equiv \sum_{n=-\infty}^{\infty} \exp\left(-\tfrac{1}{2}x^2 n^2\right) \tag{58b}$$

[note that $\beta_1(k_0) = \beta_1(2\pi/k_0)$]. Away from its minimum value $\beta_1(\sqrt{2\pi}) \cong 1.18$, $\beta_1(k_0)$ is well approximated by

$$\beta_1(k_0) \approx \frac{\sqrt{2\pi}}{k_0} + \frac{k_0}{\sqrt{2\pi}}. \tag{59}$$

Recall [cf. eq. (23)] that $|\psi_1(x, y)|^2$ is periodic on a rectangle $(\Delta x, \Delta y) = (k_0, 2\pi/k_0)$. Thus only when $k_0 = \sqrt{2\pi}$ can the $(p = 1)$ flux penetration pattern be $[x \leftrightarrow y]$ symmetric. From eqs. (57) and (59) it follows that k_0 is typically much greater or much less than $\sqrt{2\pi}$. Thus, the flux patterns will consist of *elongated* structures. Since the solution with k_0 is degenerate with its $[x \leftrightarrow y]$ version with $k_0 \leftrightarrow 2\pi/k_0$, a pattern of elongated domains is predicted.

The degree of elongation is much greater than might be expected on the basis of this simple inference. In fig. 2 flux patterns produced by $|\psi_1(x, y)|^2 \equiv \rho(x, y)$ are presented. Specifically, the shaded areas are those where ρ takes at least 0.7 of its maximum value. For $k_0 = \sqrt{2\pi} \sim 2.507$ (when $\beta_1 = 1.180$) we find fig. 2a, while for $k_0 = 1.3\sqrt{2\pi} \sim 3.259$ (when $\beta_1 = 1.326$), fig. 2b is obtained. Note that even when k_0 is slightly different from its symmetric value $\sqrt{2\pi}$, significant elongation occurs.

This is not the whole story, however. In sect. 5 an infinite set of wave functions $\psi_p(x, y)$ was defined. The above analysis concerns only $p = 1$, where the Ginzburg–Landau free energy is minimized for elongated structures. What happens for higher values of p? It will now be shown that there are always $[x \leftrightarrow y]$

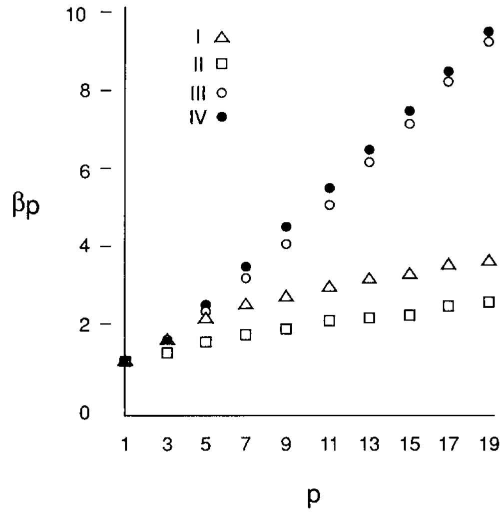

Fig. 3. Plot of $\beta_p(N)$ versus p for $N =$ I, II, III, and IV.

symmetric solutions for any $\beta \gtrsim 1.2$, but these are degenerate with a far larger number of elongated patterns. Thus, the expected pattern is highly asymmetric.

By using the notation and normalization of eqs. (25)–(28), β_p can be written

$$\beta_p = \sum_{k} |g_p(k)|^2 . \tag{60}$$

This sum has been evaluated at the symmetric point $k_0^2 = 2\pi/p$ for $C_{n/p}$ proportional to the eigenvectors $\{D_{n/p}(N),\ N = \mathrm{I, II, III, IV}\}$ of eqs. (40)–(45). The corresponding functions $\beta_p(N)$ are displayed in fig. 3.

Recall that for a given p it is possible to interpolate continuously between any two given values of $\beta_p(N)$ by taking linear combinations of the $C_{n/p}$ (with *real* coefficients). Note also that all of the β_p are monotonically increasing functions of p. [In particular, $\beta_p(\mathrm{IV}) \approx p/2$]. Thus, there is an $[x \leftrightarrow y]$ symmetric flux distribution for any given value of $\beta \gtrsim 1.2$. However, as pointed out in sect. 5, the property of $[x \leftrightarrow y]$ symmetry is highly unusual, and thus a given pattern is overwhelmingly likely to exhibit elongated flux distributions.

7. Fractal patterns

It is worth pointing out that far stranger flux patterns than the periodic Abrikosov patterns discussed above can occur. For instance, consider the continuous but nowhere differentiable function of Weierstrass [13] with fractal dimension D

$$W(t) = \sum_{n=0}^{\infty} \gamma^{(D-2)n} \cos(\gamma^n t), \tag{61}$$

which possesses the scaling property ($1 < D < 2$)

$$W(\gamma t) = \gamma^{2-D} W(t) + \cos t. \tag{62}$$

If we use $C(k) \sim W(k/L)$ in eq. (11), the result will be flux distributions which are fractal in x at scales smaller than L and consist of lumps with exponentially increasing spacing in the y-direction. The value of β for this distribution will diverge however unless $|\psi|^2$ is made space-filling.

8. Conclusions

It is clear that the superconducting intermediate state provides a fascinating laboratory for the study of unusual quantum phenomena. Unfortunately, the present analysis is severely curtailed by the limitations of perturbation theory. Recent progress in simulations of lattice Higgs models [8] suggest, however, that significant theoretical progress could soon be made in this area. (Indeed, the present work was inspired by one such simulation [9].)

Several interesting results were, however, gleaned from a perturbative analysis of the Ginzburg–Landau equations when the incident magnetic field is near its critical value. For the geometry of fig. 1, the critical superconducting wave function behaves much as if the x- and y-directions were Fourier conjugate coordinates, like position and momentum in a one-dimensional quantum mechanics problem.

It is this Fourier conjugation property of the critical wavefunction which causes the breakdown of Landau's textbook model of the intermediate state. Landau predicted [1] a field-penetration pattern which was periodic in one plane coordinate and independent of the other. Yet if a wavefunction is independent of a coordinate, its Fourier conjugate is sharply localized, not periodic.

Nevertheless, Landau's physical intuition was essentially correct. As shown above, the Ginzburg–Landau equations yield an infinite number of solutions for the flux pattern which are degenerate in free energy. The majority of the degenerate solutions are highly elongated, and so thus are the expected flux patterns. It is *symmetry breaking by indifference*—the free energy of the many elongated states equals that of the few symmetric ones, so the indifferent system usually chooses an elongated ground state.

Experimentally or in a lattice Higgs simulation this analysis suggests that in superconductors with $\kappa \lesssim 1/\sqrt{2}$ (like lead, not like aluminium) there will be a complicated and essentially unpredictable ensemble of domains containing elongated structures. These domains can be aligned by careful sample preparation, or by applying the magnetic field in a slightly oblique direction (in which case the patterns will, by the Meissner effect, align themselves parallel to the component of the magnetic field tangential to the plate). This analysis also suggests that the domains of elongated patterns meet at right angles, though this effect might depend on sample geometry.

Several interesting problems were not covered by this analysis. For simplicity, only Landau's original square plate geometry was considered, although other configurations are likely feasible. The present analysis was also concerned with only plates much thicker than the coherence length. The problem of a thin plate was addressed by Tinkham [14], Lasher [6] and others [7], who predicted that a thin enough plate gives rise to a flux pattern which is a triangular vortex array, much like a type II superconductor.

Most interestingly, questions as to the dynamics of this system (and its behavior when voltages or currents are applied) were left unanswered. It is suggestive to consider this system as a giant array of Josephson junctions with dynamic boundaries, which may have applications as diverse as a dark-matter detector for particle physics. (I am indebted to Roberto Petronzio for a discussion on this latter point).

It is a pleasure to thank Leo Stodolsky, Roberto Petronzio, and Massimo Bernaschi for many useful discussions. I also thank the Department of Energy for furnishing supercomputer time essential at various stages of this work.

References

[1] L.D. Landau, Phys. Z. Sov. 11 (1937) 129 [JETP 7 (1937) 371]; J. Phys. USSR 7 (1943) 99 [JETP 13 (1943) 377]; *in* Collected papers of L.D. Landau, ed. D. ter Haar (Gordon and Breach, New York, 1967);
L.D. Landau and E.M. Lifshitz, Electrodynamics of continuous media (Pergamon, New York, 1984) sect. 57

[2] J.D. Livingston and W. De Sorbo, *in* Superconductivity, Vol. 2, ed. R.D. Parks, (Marcel Dekker, New York, 1969);
R.P. Huebener, Magnetic flux structures in superconductors (Springer, New York, 1979);
R.N. Goren and M. Tinkham, J. Low Temp. Phys. 5 (1971) 465;
K.P. Selig and R.P. Huebener, J. Low Temp. Phys. 43 (1981) 37;
W. Buck, K.-P. Selig and J. Parisi, J. Low Temp. Phys. 45 (1981) 21

[3] Yu.V. Sharvin, Zh. Eksp. Teor. Fiz. 33 (1957) 1341 [JETP 6 (1958) 1031];
D.E. Farrell, R.P. Huebener and R.T. Kampwirth, J. Low Temp. Phys. 19 (1975) 99

[4] V.L. Ginzburg and L.D. Landau, Zh. Eksp. Teor. Fiz. 20 (1950) 1064

[5] A.A. Abrikosov, Zh. Eksp. Teor. Fiz. 32 (1957) 1442 [JETP 5 (1957) 1174];
W.H. Kleiner, L.M. Roth and S.H. Autler, Phys. Rev. 133 (1964) A122;
A.A. Abrikosov, Dokl. Acad. Nauk SSSR 86 (1952) 489

[6] G. Lasher, Phys. Rev. 154 (1967) 345; 140 (1965) A523

[7] K. Maki, Ann. Phys. (N.Y.) 34 (1965) 363;
J. Pearl, Appl. Phys. Lett. 5 (1964) 65;
A.L. Fetter and P.C. Hohenberg, Phys. Rev. 159 (1967) 330;
R.P. Huebener, Phys. Rep. C13 (1974) 143;
A. Kiendl, J. Low Temp. Phys. 38 (1980) 277;
D.J.E. Callaway, Rockefeller University preprint, RU89/B1/47, to appear in Nucl. Phys. B (Proc. Suppl.)
[8] P.H. Damgaard and U.M. Heller, Phys. Rev. Lett. 60 (1988) 1246;
D.J.E. Callaway and L.J. Carson, Phys. Rev. D25 (1982) 531;
D.J.E. Callaway and R. Petronzio, Nucl. Phys. B240 [FS18] (1987) 481
[9] M. Bernaschi, R. Petronzio and L. Stodolsky, unpublished
[10] S. Weinberg, Prog. Theor. Phys. Suppl. 86 (1986) 43
[11] L.P. Gor'kov, Zh. Eksp. Teor. Fiz. 36 (1959) 1918 [Sov. Phys. JETP 9 (1959) 1364]
[12] E. Wigner, Phys. Rev. 40 (1932) 749
[13] K. Weierstrass, Mathematische Werke (Mayer and Muller, Berlin, 1895);
B.B. Mandelbrot, Les objects fractals (Flammarion, Paris, 1975); Fractals: Form, chance, and dimension (Freeman, San Francisco, 1977); The fractal geometry of nature (Freeman, San Francisco, 1982);
M.V. Berry and Z.V. Lewis, Proc. R. Soc. London A370 (1980) 459; T. Tél, Z. Naturforsch. 43a (1988) 1154
[14] M. Tinkham, Phys. Rev. 129 (1963) 2413; Rev. Mod. Phys. 36 (1964) 268
[15] E. Weinberg, Phys. Rev. D19 (1978) 3008
[16] E.B. Bogmol'nyi, Yad. Fiz. 24 (1976) 861 [Sov. J. Nucl. Phys. 24 (1976) 449];
H. de Vega and F. Schaposnik, Phys. Rev. D14 (1976) 1100;
L. Jacobs and C. Rebbi, Phys. Rev. B19 (1978) 4486